Light, oxygen, voltage (LOV) domains represent the key sensory modules of blue-light photoreceptor proteins widely distributed in all kingdoms of life. Although LOV proteins possess a structurally conserved core domain, they differ significantly in the N- and C-terminal elements that largely determine the mode of dimerization. Limited information is currently available regarding any light-dependent quaternary structural changes, although a light-dependent alteration of the monomer-dimer equilibrium would represent a feasible mode of signal-relay for 'short' LOV proteins, where one of the two quaternary structural states selectively mediates the interaction with downstream signaling partners, triggering the cellular response. We previously determined the crystal structure of two such short LOV proteins, namely PpSB1-LOV of Pseudomonas putida and DsLOV of Dinoroseobacter shibae.

For DsLOV, our previous SAXS measurements verified the mode of dimerization as seen in the dark-state crystal structure. The objective of the experiment was to characterize the overall quaternary structure, monomer:dimer equilibrium and the low-resolution shape of both the dark- and the light-state of several LOV proteins in solution. In this proposal, we aimed to measure selected LOV proteins in dark and light adapted states using the SAXS technique. These proteins exhibit dark recovery time in the range from seconds (fast reverting) to days (slow reverting). The photochemical properties of the proteins selected for these studies have been determined in our group: PpSB1-LOV (lifetime of the photo-adduct $\tau_{REC} \approx 2500$ min, 20 °C), PpSB1-LOV-R61H/R66I ($\tau_{REC} = 9$ min), DsLOV-M49I ($\tau_{REC} = 2.6$ min), YF1 ($\tau_{REC} =$ 93 min) and SB1F1 ($\tau_{REC} = 923$ min).

In the following we present the key results obtained from the experiment on BM29:

In general the static dark and light SAXS experiments worked well and gave valuable information about the possible signal transfer mechanism of PpSB1.

We were able to record time-resolved SAXS data with a delay time of several minutes from the light illuminated state through the recovery process to the fully dark adapted state. However, the kinetic SAXS experiments did not show any significant and statistically relevant differences in the recorded diffractograms. We attribute that result to the not perfect illumination of the sample and the fact that the light state could not be excited for the kinetic experiments. In a following SAXS experiment on BM29 we would like to repeat the time-resolved SAXS experiments, which would give valuable information who the light-state returns structurally to the dark-state.

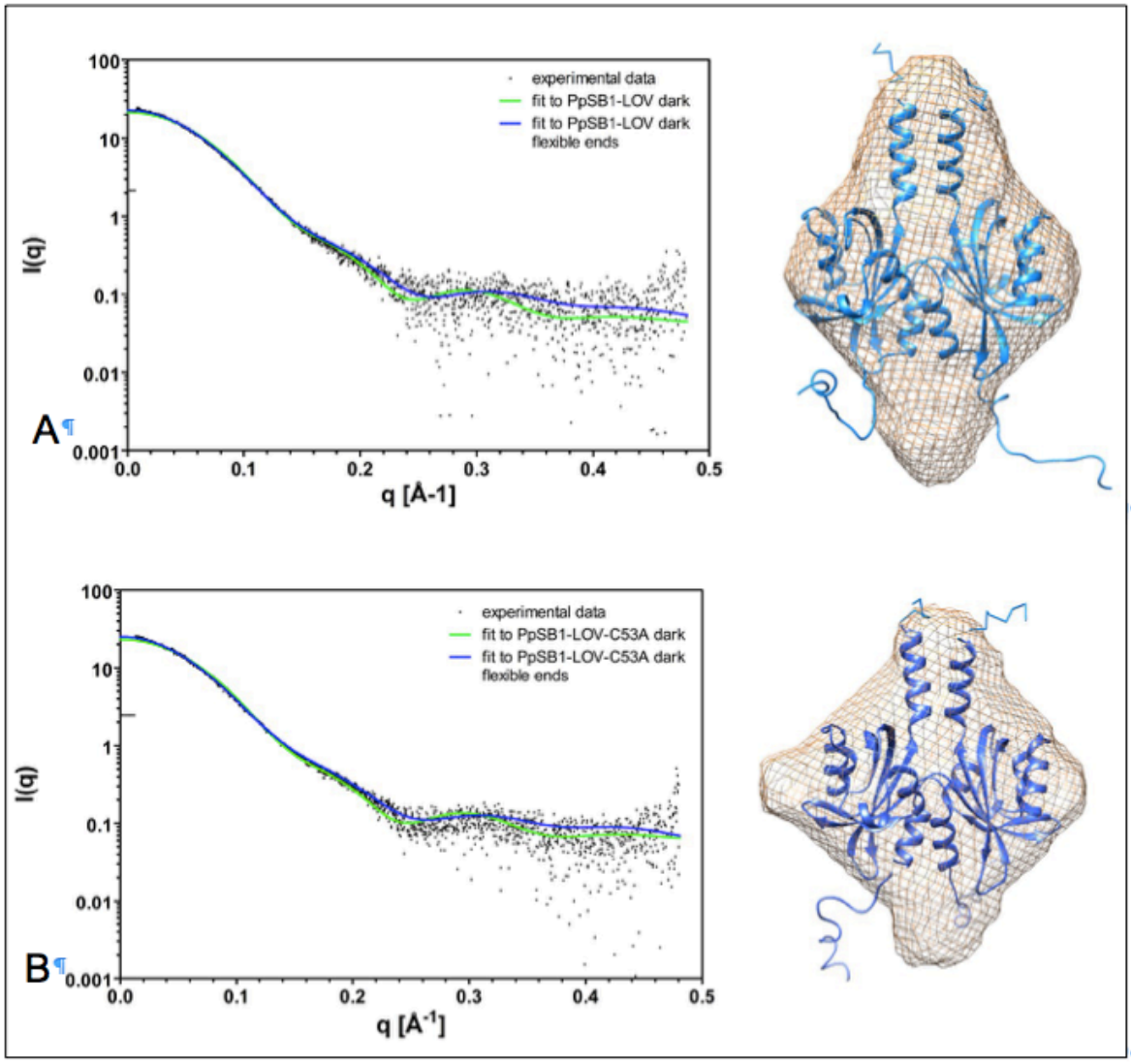

Figure 1: Small angle X-ray scattering of dark state PpSB1-LOV (A), PpSB1-LOV-C53A (B). The calculated curves of the respective dark state crystal structures (green) are fitted to the experimental SAXS data (black dots). In the crystal structure a decent number of C- and N-terminal amino acid residues are missing as no electron density was observed. These amino acids still contribute to the solution scattering data and therefor dummy atoms were modeled C- and N-terminally to the crystal structure using the program CORAL **(Petoukhov , et al., 2012)**. Subsequently, calculated curves of the crystal structures with the introduced flexible ends (green) were equally fitted to the experimental data. Additionally, the *ab initio* models (orange shown in mesh) of each structure are aligned with the crystal structures including the flexible ends (blue ribbon representation).

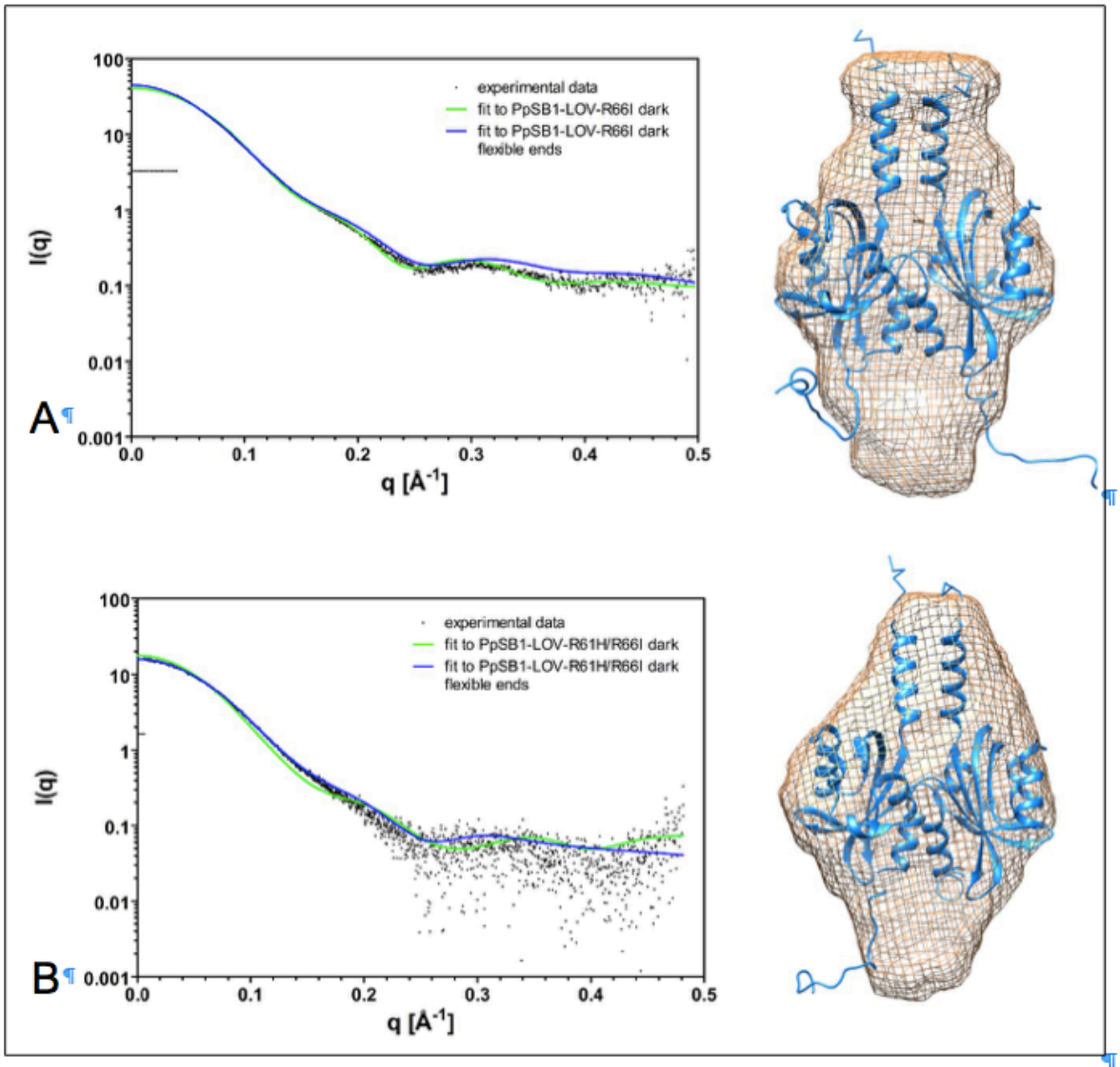

Figure 2: Small angle X-ray scattering of dark state PpSB1-LOV-R66I (A), PpSB1-LOV-R61H/R66I (B). The calculated curves of the respective dark state crystal structures (green) are fitted to the experimental SAXS data (black dots). In the crystal structure a decent number of C- and N-terminal amino acid residues are missing as no electron density was observed. These amino acids still contribute to the solution scattering data and therefor dummy atoms were modeled C- and N-terminally to the crystal structure using the program CORAL **(Petoukhov , et al., 2012)**. Subsequently, calculated curves of the crystal structures with the introduced flexible ends (green) were equally fitted to the experimental data. Additionally, the *ab initio* models (orange shown in mesh) of each structure are aligned with the crystal structures including the flexible ends (blue ribbon representation).

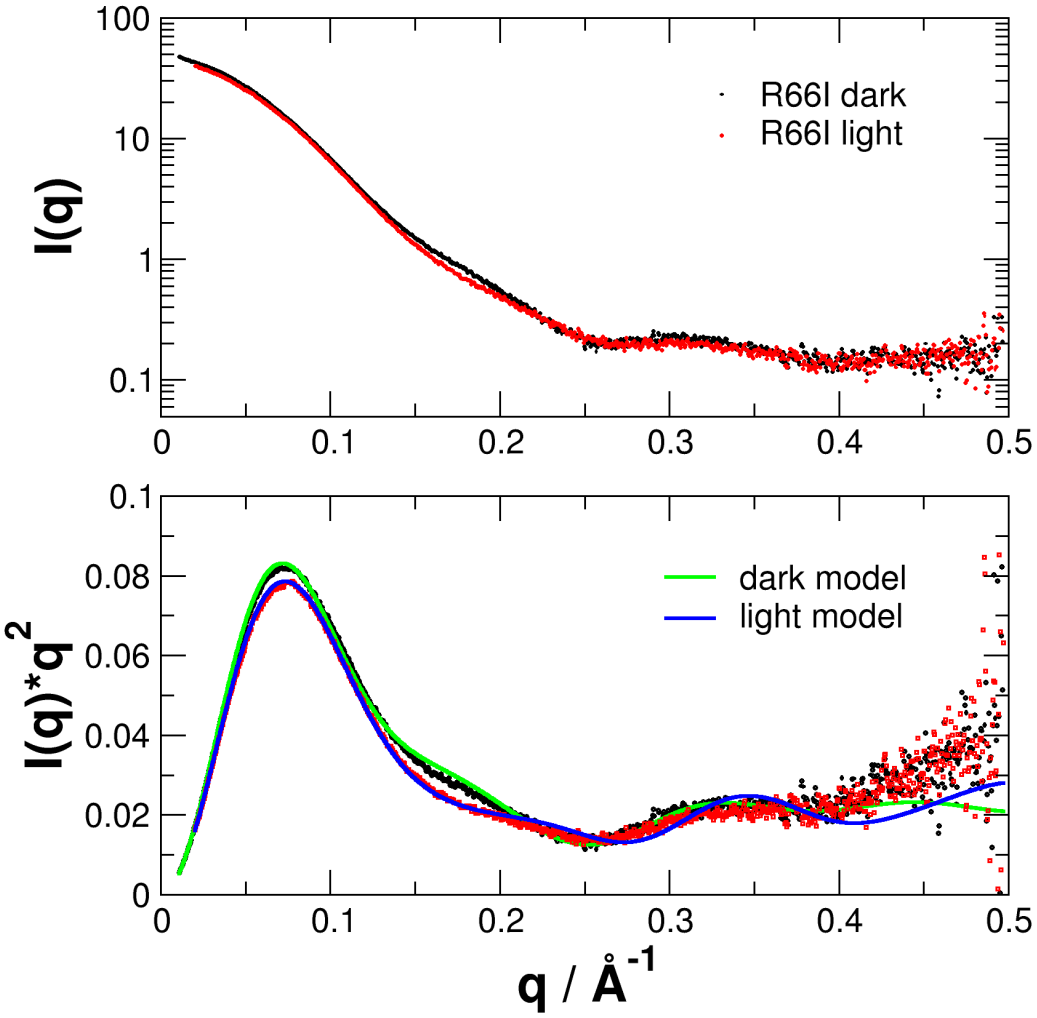

Figure 3: SAXS data of PpSB1-R66I in the dark adapted state and the blue light illuminated state. A difference in the measured SAXS data between 0.1 and 0.2 $Å^{-1}$ is visible with the eye. On the bottom the data are plotted as Kratky plots. The solid green and blue lines are calculated curves of models determined with the CORAL program. The observed differences mainly stem from ordered and disordered end regions at the top of the long Jα helices.

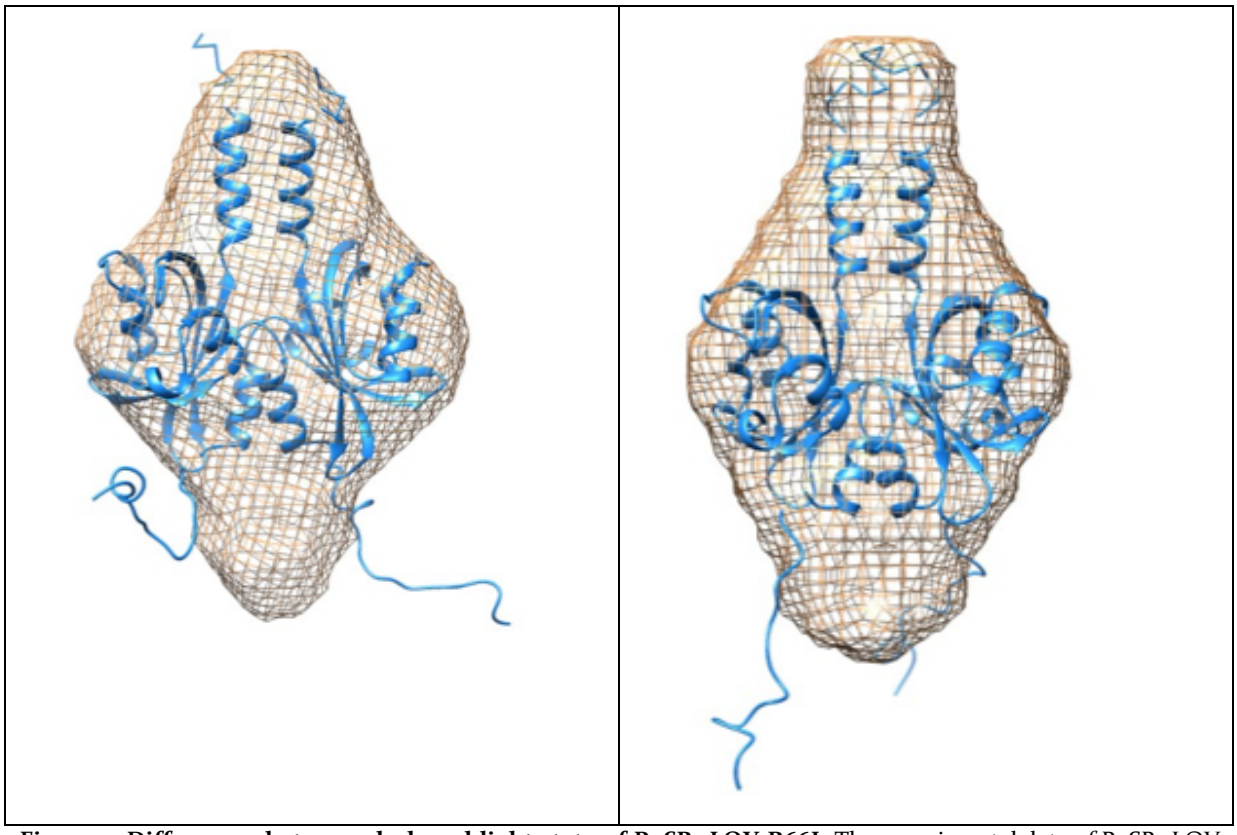

Figure 4: Differences between dark and light state of PpSB1-LOV-R66I. The experimental data of PpSB1-LOV-R66I in dark state (filled dots) are shown in combination with the calculated curve of the crystal structure of PpSB1-LOV (green line) and with the calculated curve of the crystal structure of PpSB1-LOV with flexible ends (blue line) and the *ab initio* models (blue in ribbon representation, shown in orange mesh) of each structure are aligned with the crystal structure of PpSB1-LOV dark state including the flexible ends. The same results are shown in (B) for the light state structure. Note that the main difference of the light and dark states are the ordered and disordered end regions of the long Jα.

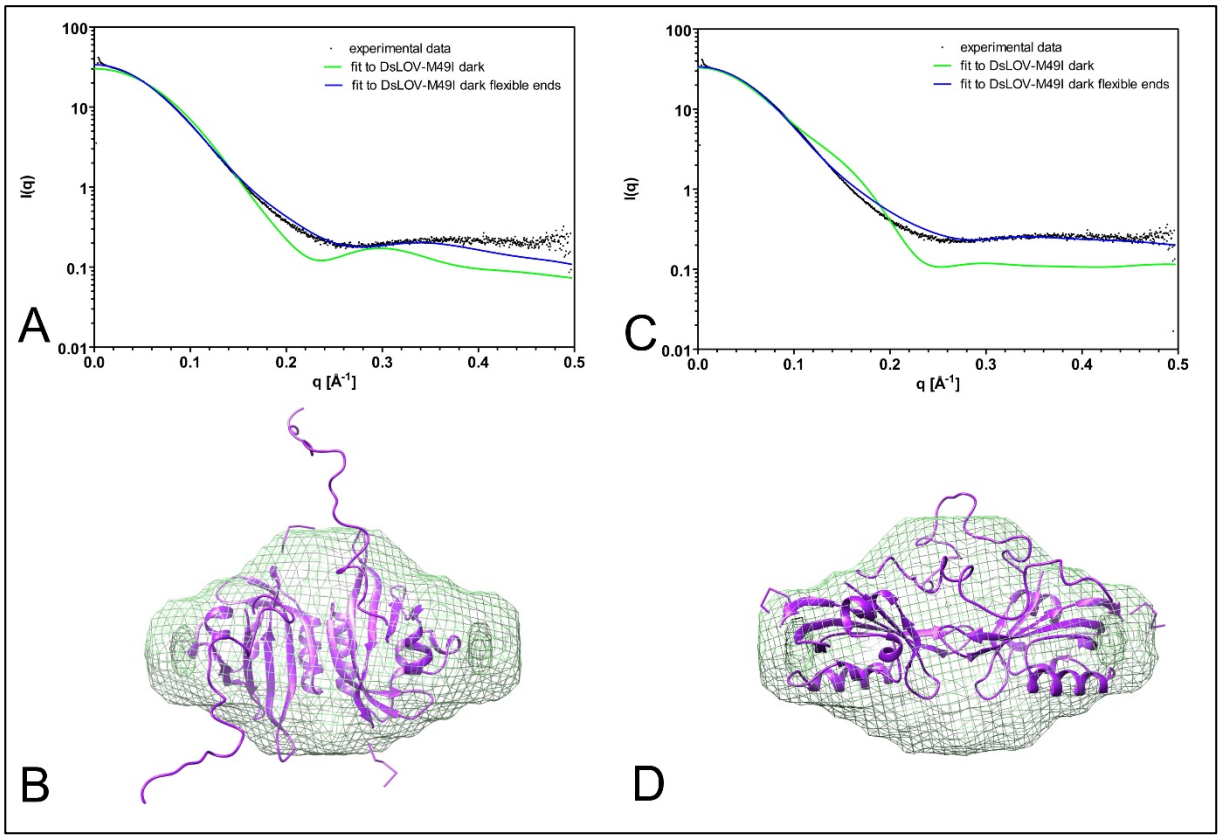

Figure 5: Small angle X-ray scattering of DsLOV-M49I dark state. (A)The experimental data (filled dots) are shown in combination with the calculated curve of the crystal structure of DsLOV-M49I β-sheet dimer (green line) and with the calculated curve of the crystal structure β-sheet dimer with flexible ends (blue lines). (B) The crystal structure of DsLOV-M49I (β-sheet dimer) in ribbon representation (purple) is aligned to the *ab initio* model in mesh(blue). (C)The experimental data (filled dots) are shown in combination with the calculated curve of the generated N-cap dimer structure of DsLOV-M49I (green line) and with the calculated curve of the equal dimer structure with flexible ends (blue lines). (D) The crystal structure of DsLOV-M49I (N-cap dimer) in ribbon representation (purple) is aligned to the *ab initio* model in mesh(blue).

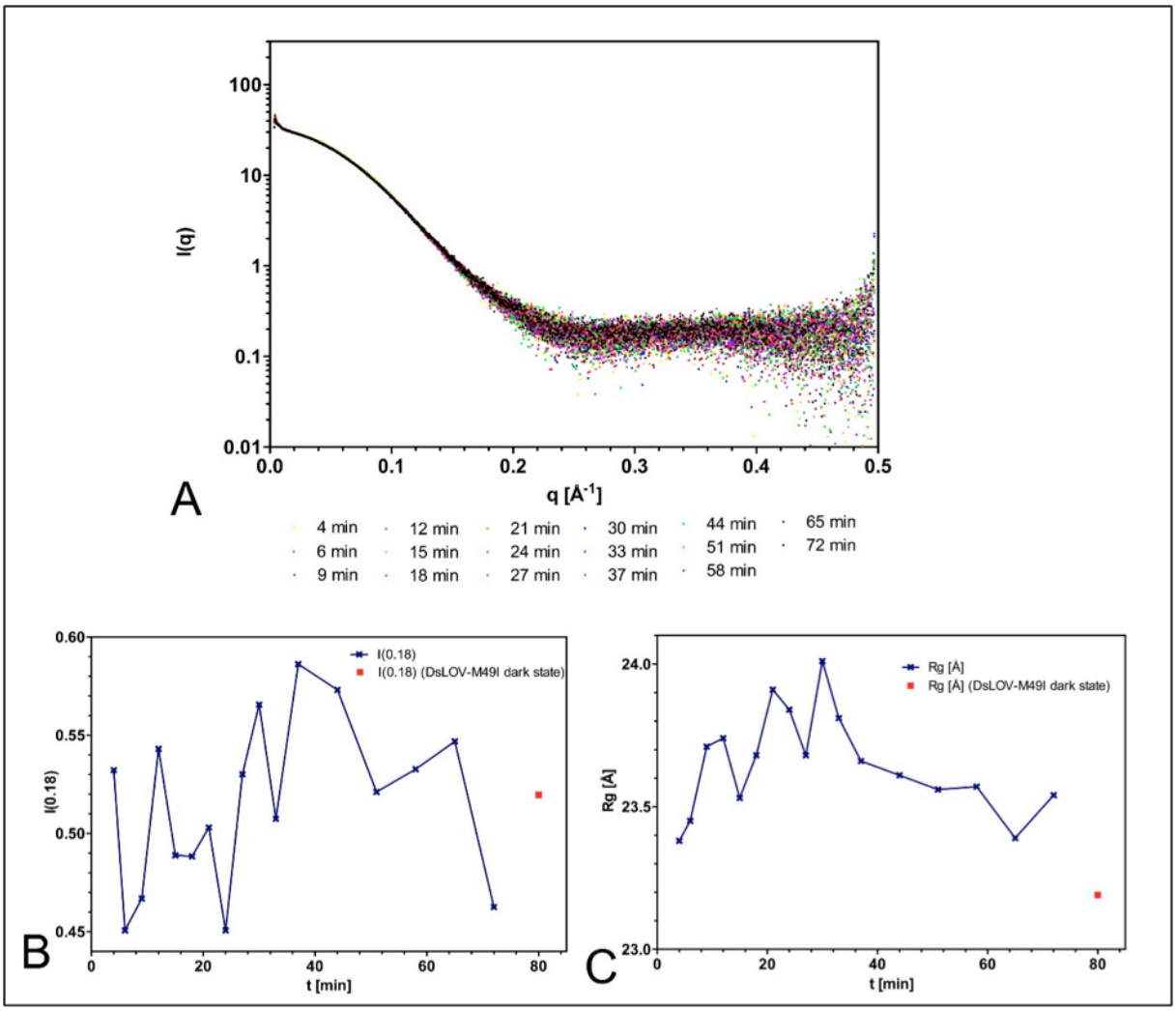

Figure 6: Kinetic measurements of DsLOV-M49I. (A) Scattering curves at different time points during dark recovery of DsLOV-M49I; (B) Time-dependent changes of the scattering intensity at q = 0.18 Å^{-1}, where the differences in the static measurements between dark and light state of PpSB1-LOV-R66I were observed, the intensities of the static dark state measurements of DsLOV-M49I are highlighted in pink; (C) Time-dependent changes of the radius of gyration during the dark recovery, the intensities of the static dark state measurements are highlighted in pink

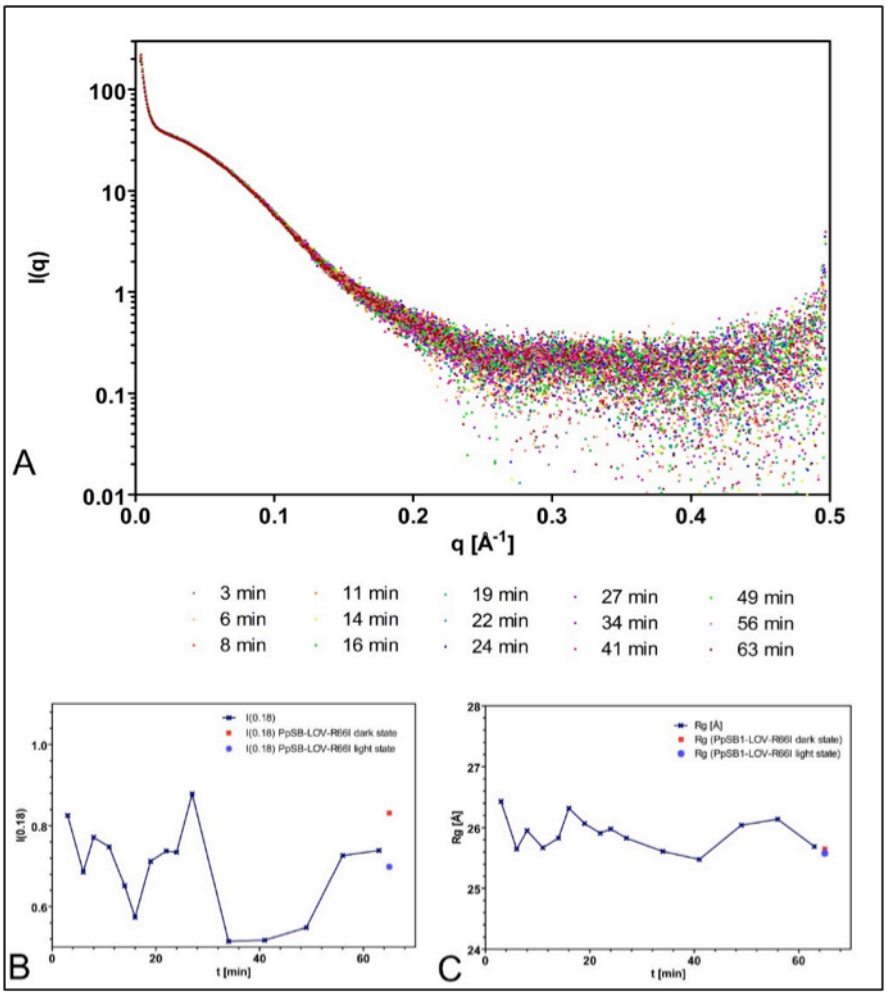

Figure 7: Kinetic measurements of PpSB1-LOV-R66I. (A) Scattering curves at different time points during dark recovery of PpSB1-LOV-R66I; (B) Time-dependent changes of the scattering intensity at q = 0.18 $Å^{-1}$, where the differences in the static measurements between dark and light state were observed, the intensities of the static dark and light state measurements are highlighted in pink and blue respectively; (C) Time-dependent changes of the radius of gyration during the dark recovery, the intensities of the static dark and light state measurements are highlighted in pink and blue respectively.